Journal of Colloid and Interface Science 437 (2015) 111–118

Contents lists available at ScienceDirect

Journal of Colloid and Interface Science

www.elsevier.com/locate/jcis

Neuropeptide Y and its *C*-terminal fragments acting on Y_2 receptor: Raman and SERS spectroscopy studies

Helena Domin [a], Ewa Pięta [b], Natalia Piergies [b], Dominika Święch [b], Younkyoo Kim [c], Leonard M. Proniewicz [b], Edyta Proniewicz [d,*]

[a] *Department of Neurobiology, Institute of Pharmacology, Polish Academy of Sciences, Smętna 12, 31-343 Kraków, Poland*
[b] *Faculty of Chemistry, Jagiellonian University, ul. Ingardena 3, 30-060 Kraków, Poland*
[c] *Department of Chemistry, Hankuk University of Foreign Studies, Yongin, Kyunggi-Do 449-791, Republic of Korea*
[d] *Faculty of Foundry Engineering, AGH University of Science and Technology, ul. Reymonta 23, 30-059 Kraków, Poland*

ARTICLE INFO

Article history:
Received 25 August 2014
Accepted 19 September 2014
Available online 28 September 2014

Keywords:
Raman spectroscopy, RS
Surface-enhanced Raman Spectroscopy, SERS
Neuropeptide Y, NPY
Silver colloid
Y_2 receptor agonist
Native and mutated *C*-terminal NPY fragments

ABSTRACT

In this paper, we present spectroscopic studies of neuropeptide Y (NPY) and its native NPY^{3-36}, NPY^{13-36}, and NPY^{22-36} and mutated acetyl-($Leu^{28,31}$)-NPY^{24-36} *C*-terminal fragments acting on Y_2 receptor. Since there is some evidence for the correlation between the SERS patterns and the receptor binding ability, we performed a detailed analysis for these compounds at the metal/water interface using Raman spectroscopy (RS) and surface-enhanced Raman spectroscopy (SERS) methods. Many studies have suggested that interactions of this kind are crucial for a variety of biomedical and biochemical phenomena. The identification of amino acids in these peptide sequences by SERS allowed us to determine which molecular fragments were responsible for the interaction with the silver nanoparticle surface. Our findings demonstrated that in all of the investigated compounds, the NPY^{32-36} *C*-terminal fragment (Thr^{32}–Arg^{33}–Gln^{34}–Arg^{35}–$Tyr^{36}NH_2$) was involved in the adsorption process onto metal substrate. The results of the present study suggest that the same molecular fragment interacts with the Y_2 receptor, what proved the usefulness of the SERS method in the study of these biologically active compounds. The search for analogs acting on Y_2 receptor may be important from the viewpoint of possible future clinical applications.

1. Introduction

Neuropeptide Y (NPY) is a highly conserved 36 amino acid peptide that plays the role of a neurotransmitter and neuromodulator (see Fig. 1 for the primary structure of porcine and bovine NPY; human, rat, guinea, and rabbit NPY contain Met instead of Leu at position 17 in the amino acid sequence (Leu^{17})) [1,2]. NPY is present in the central and peripheral neurons and is described as one of the most abundant peptides in the brain [3]. This peptide is involved in many physiological functions, including the regulation of blood pressure (in the periphery NPY is a potent vasoconstrictor), cardiorespiratory parameters, body temperature, feeding, sexual behavior, pain, anxiety (NPY has a strong antianxiety effect), neuronal activity (it reduces epileptiform activity in the hippocampus by inhibition of glutamate release), circadian rhythms, and memory process [4]. It also controls the release of luteinizing hormone releasing hormone (LHRH) and corticotrophin releasing factor (CRF) [5].

The aforementioned numerous and diverse actions of NPY are mediated by G-protein-coupled receptors (GPCRs) denoted as Y_1, Y_2, Y_3, Y_4, Y_5, and Y_6 [6]. GPCRs are a superfamily of integral membrane proteins characterized by seven α-helical fragments (7TM) that span the cellular membrane [7]. Five of them, except Y_3, have been cloned [4]. Among the NPY receptors, the Y_1, Y_2, and Y_5 receptors have been postulated to be the most important in the regulation of neurotoxicity and neuroprotection [8]. However, the most promising neuroprotective effect was observed after Y_2 receptor stimulation [8]. Since specific agonists and antagonists of the Y_2 receptor have been synthesized [9,10], the studies on the role of this receptor subtype in neuroprotection became possible. Our earlier study has shown that the Y_2 receptor agonist NPY^{13-36} induces neuroprotective effects against kainate-induced excitotoxicity both *in vitro*, in the primary cortical and hippocampal cultures of mouse neurons, and *in vivo*, after intrahippocampal injections in rats [8]. Although a large number of substances have been studied and found to be neuroprotective in animal stroke models, the

* Corresponding author. Fax: +48 12 633 6348.
E-mail address: proniewi@agh.edu.pl (E. Proniewicz).

http://dx.doi.org/10.1016/j.jcis.2014.09.053
0021-9797/

results of clinical trials have been unsuccessful. Therefore, the search for modified analogues acting on the Y_2 receptor that cross the blood–brain barrier are important from the point of view of possible future clinical applications.

In the literature, the three-dimensional structure of positively charged NPY in an aqueous solution, in the presence of organic solvents (dimethyl sulfoxide, DMSO; 2,2,2-trifluoroethanol, TFE; hexafluoro-2-propanol, HFIP), and in membrane mimetic micelles (dodecylphosphocholine, DPC) has been controversially proposed [11,12]. Generally, two classes of molecular conformations of NPY were predicted. NPY belongs to the pancreatic polypeptide family (PP family); thus, based on homology of the primary structure of NPY with that of avian pancreatic polypeptide (APP) for which the X-ray crystallography data are available [13], the first class model (from 1980's) has assumed a common hairpin-like fold (the PP-fold) structure of NPY [13,14]. This hairpin-like tertiary structure consists of an *N*-terminal extended type II polyproline helix (residues 1–8) followed by a turn (residues 9–13) and an amphipathic α-helix (residues 14–32) [15,16]. In this model, a strong hydrophobic interaction between the α-helix and slightly amphiphilic polyproline helix has been suggested [15]. The *C*-terminal end has been supposed to adopt a flexible turn structure projecting away from the hairpin loop. The second more recent (from late 1980s and 1990s) model of the NPY conformation is based on the NMR and CD spectroscopic data and molecular dynamics simulation [2,17–19]. In this model, the 11–36 (in water) and 19–34 (in TFE) *C*-terminal NPY fragments adopt the amphiphilic α-helical structure, whereas the *N*-terminal part of the molecule is fully flexible with no regular structure (see Fig. 1) [2]. The results obtained for NPY in highly diluted aqueous solution and for NPY in the TFE solvent have shown that this peptide exists in a monomeric form [20]. The packing of the monomer is obtained mainly via the Tyr and Ile side-chain interactions of hydrophobic character [21]. Additionally, Cowley et al. [21] and Monks and co-workers [2] have found that NPY in water as well as in the absence of the membrane mimetic micelles and receptors undergoes self-association. The formation of the dimeric species depends on the hydrophobic residues (Leu^{17}, Tyr^{21}, Leu^{24}, Ile^{28}, Leu^{30}, Ile^{31}, and Thr^{32}) located at the inner side of the curved α-helix that are aligned in a parallel and antiparallel manner [21]. At the dimer interface, the protons of the amide bonds are either protected from exchange with water or are involved in hydrogen-bonding [21]. On the other hand, in the presence of a lipid membrane, the interactions of NPY with the hydrophobic regions of the membrane are favored over hydrophobic packing in the dimer. Therefore, the dimer is not expected to be physiologically relevant to the binding to the receptor. During the binding of NPY to the lipid membrane surface, a conformational reorientation of the Thr^{32}–$Tyr^{36}NH_2$ segment occurs. This particular fragment, consisting of the Arg^{33} and Arg^{35} residues, is believed to directly, probably via electrostatic attraction, interact with the receptor [22]. At the lipid/water interface, the *C*-terminal α-helix of NPY adopts the parallel orientation to the membrane surface and penetrates the hydrophobic interior only through the hydrophobic residues that possess the long side-chains and face toward the micelle surface [23]. Therefore, it has been suggested that the NPY dimer interface is relevant to the NPY monomer/DPC interface that is formed through hydrophobic rather than electrostatic interactions [23]. However, the exact arrangement of NPY in respect to the membrane might additionally depend on the local electropotential [24]. It has been also proven that the mobile *N*-segment does not interact with the micelles [2,25].

The aforementioned implications of the NPY conformation for the receptor recognition are important for determination of the structure–function relationship of NPY and its analogues acting on the Y_2 receptors. The studies have shown that the *C*-terminus of NPY, especially Leu^{30}–Tyr^{36} fragment that is conserved in all the Y_2 agonists, is a common recognition site for the receptor binding [26]. Amino acid substitutions in this region have several subtype-specific effects on ligand binding affinity. For example, any exchange of Arg^{33} considerably reduces ligand binding to the Y_2 receptor. The $Arg^{35} \rightarrow Ala^{35}$ substitution produces a complete loss of affinity at all Y receptor subtypes. Replacement of the Tyr^{20}, Leu^{24}, Tyr^{27}, and Leu^{30} residues in the α-helix with polar residues destabilizes the NPY structure, whereas replacement of external residues (Arg^{19}, Ser^{22}, and His^{26}) has no effect on the ligand binding; however, it may alter the solvent-accessible surface [15]. Deamidation of the $Tyr^{36}NH_2$ or deletion of $Tyr^{36}NH_2$ results in complete loss of the NPY activity. The *N*-terminal fragment is completely inactive in respect of the Y_2 receptors [11].

In this paper, we focused on determination of the structure and adsorption geometry of the porcine NPY and its native NPY^{3-36}, NPY^{13-36}, and NPY^{22-36} and mutated acetyl-$(Leu^{28,31})$-NPY^{24-36} *C*-terminal fragments immobilized at the metal/water interface, by means of Raman and surface-enhanced Raman (SERS) spectroscopies. The Raman spectroscopy is the best tool for analyzing the biologically active compounds because it provides full vibrational characterization of the investigated molecules in their natural environment (an aqueous solution, pH = 7) [27]. This non-destructive and non-invasive method is commonly used to study many biological systems, such as identification of bacteria and viruses [28–30], peptide interactions [29], or elucidation of the protein secondary structure [31]. However, the low Raman scattering cross-section limits its applications [27]. The enormous enhancement of the Raman signal can be achieved by use the SERS technique for a molecule located on or near metal surface [32]. Thus, it is possible to perform measurements at a very low peptide concentration that is extremely important in terms of biological materials. The SERS phenomenon allows for deduction of the possible metal surface/molecule interactions [33]. These interactions can be detected for specific peptide regions that are either in close proximity or adsorbed onto a metal surface. Consequently, analysis of the SERS signals (wavenumber, enhancement, and broadness) from the amino acids in the peptide sequence is crucial to describe how a peptide can interact with the surrounding medium [34–36]. As a result, it could shed some light on the *in vivo* behavior of the molecule [37].

The general aim of this study was to investigate the adsorption geometry of NPY and its native NPY^{3-36}, NPY^{13-36}, and NPY^{22-36} and mutated acetyl-$(Leu^{28,31})$-NPY^{24-36} *C*-terminal fragments onto colloidal silver nanoparticles. In particular, we focused on determination which molecular fragments are responsible for the interaction of the peptide at the physiological conditions with the silver nanoparticle surface. NPY^{13-36} and NPY^{22-36} were chosen because NPY^{22-36} retains subnanomolar affinity for the Y_2 receptor, whereas NPY^{13-36} exists (in 30% HFIP) as the fully α-helical monomer [22]. The endogenous porcine NPY^{3-36} fragment has similar high affinity for the Y_2 receptors as NPY and is responsible for 35% of NPY immunoreactivity in the porcine brain. Thus, the *N*-terminal deletion of the Tyr^1-Pro^2 dimer converts an unselective Y_1/Y_2 receptor ligand into a highly Y_2 selective ligand [38]. On the other hand, the acetyl-$(Leu^{28,31})$-NPY^{24-36} analogue is the potent Y_2 receptor agonist present as the unordered monomer in the aqueous solution, whereas in 40% THF its 25–35 residues form the well-defined helical structure [39].

The information obtained from the SERS analysis was compared with the biological activity studies [40,41], which identified the molecular fragments of NPY involved in the receptor binding (see the above paragraphs). The contribution of the structural components to the ability to interact with the Y_2 receptor was correlated with the SERS patterns. By this, we proved the usefulness of the SERS technique in the study of the biologically active compounds.

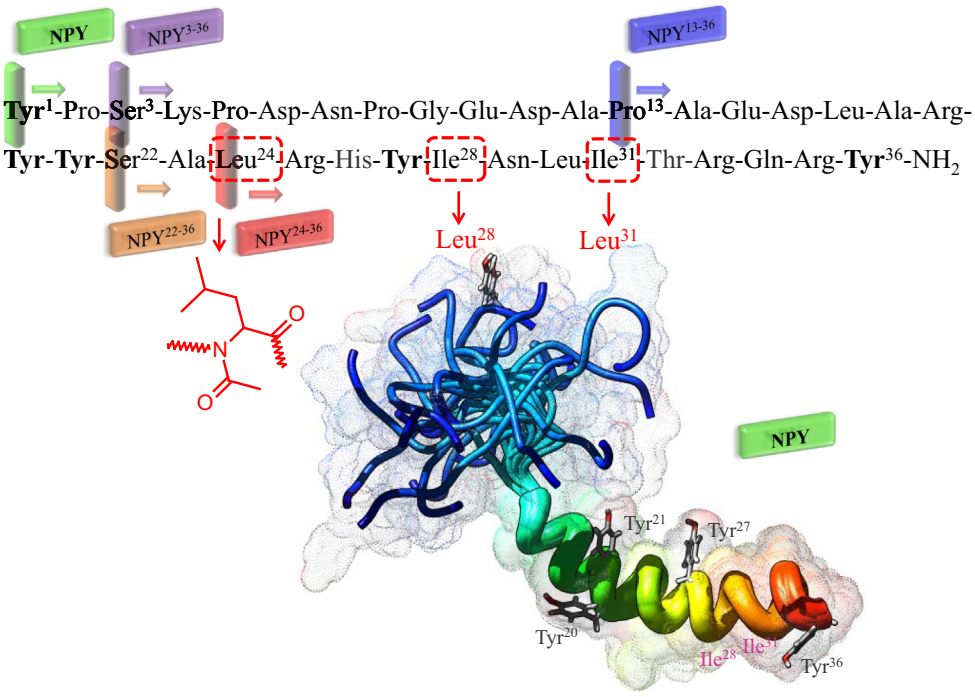

Fig. 1. Amino acid sequence and secondary structure (1RON.pdb from PDB)[2] of porcine NPY monomer together with its marked NPY$^{3-36}$, NPY$^{13-36}$, and NPY$^{22-36}$ *C*-terminal fragments and acetyl-(Leu^{28,31})-NPY$^{24-36}$ analogue.

2. Experimental

2.1. Peptides

Porcine neuropeptide Y and its 13–36 (NPY$^{13-36}$) were purchased from Tocris Bioscience (UK). Native 3–36 (NPY$^{3-36}$) and 22–36 (NPY$^{22-36}$) fragments from porcine neuropeptide Y and mutated acetyl-(Leu^{28,31})-neuropeptide Y 24–36 fragment (acetyl-(Leu^{28,31})-NPY$^{24-36}$) were purchased from Bachem Co. (Switzerland).

2.2. Raman spectra measurements

Due to a very small amount of samples, the RS spectra were obtained for each solid peptide placed on a glass plate. For NPY$^{13-36}$ of the highest quantity, the RS spectrum in an aqueous solution was measured. The spectra were recorded on a InVia Raman microscope (Renishaw, England) equipped with CCD detector and the confocal microscope Leica with a 100× magnification objective. The spectral resolution was set at 2 cm^{-1}. 785 nm line from a diode laser (HPNIR, Renishaw) was used as an excitation source. The laser power at the output was set at 30 mW. Typically, 4 scans were collected.

2.3. UV–vis measurements

The UV–vis spectra of the silver sol and protein/silver sol systems (1 h after mixing) (see Fig. 2) were recorded on a Thermo Scientific (model EVO-60) spectrophotometer.

2.4. SERS spectra measurements

An aqueous solutions of the investigated peptides were prepared by dissolving of each peptide in deionized water to the 10^{-4} M peptide concentration. Silver sol (silver particle size: 20 nm; concentration: 0.02 mg/ml in an aqueous buffer, containing sodium citrate as stabilizer) was purchased from Sigma (Poland). 20 μl of each peptide solution was added to 40 μl of the silver sol and the measurement was performed after 1 h of mixing.

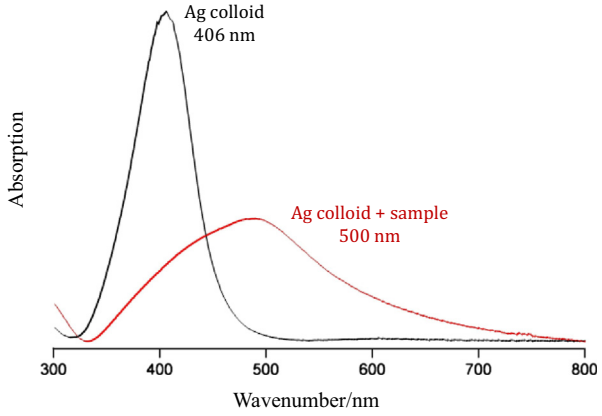

Fig. 2. Excitation spectra (UV–vis) of an aqueous silver colloid and sample/silver nanoparticle system used in this study.

The SERS spectra were recorded on the same spectrometer as the RS spectra. However, during the measurements a 50× long distance magnification objective was used. Typically, the SERS spectra were recorded at three spots on the surfaces of the colloidal silver nanoparticles. The spectra from the series were nearly identical, except for small changes (up to 5%) in some band intensities. No spectral changes associated with the sample decomposition or desorption process were observed.

3. Results and discussion

Fig. 3 shows the RS spectra of solid porcine NPY and its native NPY$^{3-36}$, NPY$^{13-36}$, and NPY$^{22-36}$ and modified acetyl-(Leu^{28,31})-NPY$^{24-36}$ *C*-terminal fragments. As can been seen from this figure,

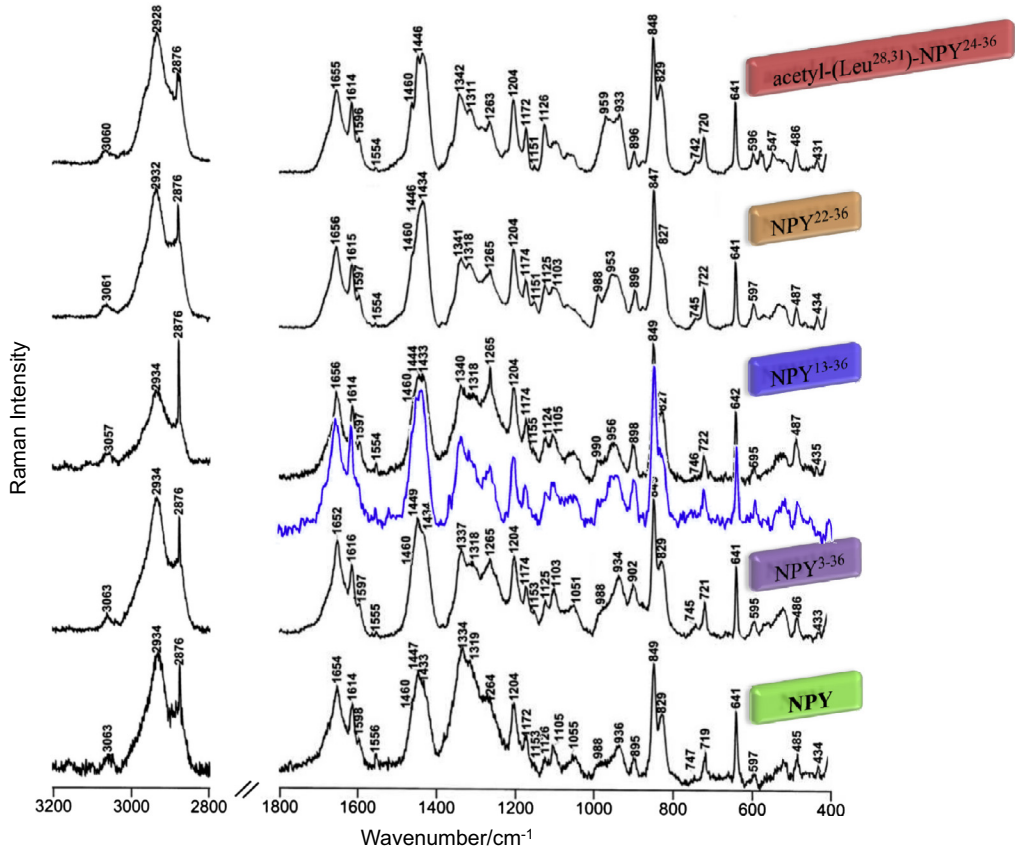

Fig. 3. The RS spectra porcine NPY and its native NPY^{3-36}, NPY^{13-36}, and NPY^{22-36} and mutated acetyl-$(Leu^{28,31})$-NPY^{24-36} *C*-terminal fragments (blue line trace – the RS spectrum of NPY^{13-36} in an aqueous solution). (For interpretation of the references to color in this figure legend, the reader is referred to the web version of this article.)

spectra of the solid porcine NPY (Fig. 3, the bottom trace) and its 13–36 fragment (Fig. 3, black line trace) are much like the Raman spectra of synthetic NPY (475–1775 cm^{-1} spectral range) [17] and NPY^{13-36} in an aqueous solution (Fig. 3, blue line trace), respectively. This similarity is not surprising since it has been proven that many peptides do not change their structures upon transition from the solid state to aqueous solution, except for extreme pH conditions [35]. However, an intensity ratio of a Tyr doublet at 828/850 cm^{-1} (NPY contains 5 Tyr residues in its primary structure), due to a Fermi resonance between the ring-breathing vibrations and an overtone of an out-of-plane ring bending of the *para*-substituted benzene ring of Tyr [42], is determined by the nature of the hydrogen-bonding of the phenolic hydroxyl in the Tyr residue ($I_{830/850} > 1$ for "buried" Tyr (the hydroxyl group is strongly hydrogen bonded to a negative acceptor); $I_{830/850} < 1$ for "exposed" Tyr (the hydrogen-bonding is weaker or an acidic external proton is bonded to the oxygen of the phenolic hydroxyl moiety) and thus, can vary upon an alternation of experimental conditions [43]. In the RS spectra of both lyophilized porcine NPY/NPY^{13-36} and synthetic NPY/NPY^{13-36} dissolved in water, the higher-frequency band from the Tyr doublet is stronger than that at the lower frequency. Therefore, based on the intensity ratio of this doublet, it can be concluded that the number of Tyr residues exposed to the hydrophilic environment ($Tyr^{1,36}$) and the number of Tyr embedded in hydrophobic globin ($Tyr^{20,21,28}$) is similar for solid peptides ($I_{830/850}$ equal 0.5–0.6) and peptides in solution ($I_{830/850}$ equal 0.4–0.5). Therefore, the RS spectra of the investigated peptides were shown for the solid state and were further used for analysis of the respective SERS spectra of peptides in the silver sol that are presented in Fig. 4. The wavenumbers of enhanced bands in RS and SERS spectra, together with their proposed assignment [17,42–62], are summarized in Table 1.

As expected, the RS spectra of all the investigated peptides (Fig. 3) are dominated by the characteristic Raman signals caused by the Tyr residue vibrations. Briefly, modes of these vibrations show comparable relative intensities and wavenumbers between the spectra; i.e., 3063–3057 [ν_2], 1616–1614 [ν_{8a}], 1598–1596 [ν_{8b}], ~1434 [ν_{19b}], 1342–1334 [ρ_{ipb}(CH) + ν_{trig}(CC), ν(CO)], 1204 [ν_{7a}], 1174–1172 [ν_{9a}, ρ_{ipb}(CH)+ $\nu(C_6H_5—C)$, $\nu_{sym}(C_\beta C_\gamma H_2 C_\delta)$], 1105–1103 [$\rho_w$(CH)], 936–933 [$\nu_5$], 902–895 [$\rho_r(C_\gamma H_2)$], 849–847 [doublet (CCC puckering)], 829–827 [doublet (trigonal CCC bend)], 722–719 [ν_4], 642–641 [ν_{6b}], and 435–431 cm^{-1} [ν_{6a}] (see Table 1 for precise band wavenumbers and assignments). However, some differences in the relative intensities of the overlapped bands are observed in the spectral range of 990–890 cm^{-1}. These differences are attributed to the contribution of the Raman scattering arising from the aliphatic side-chain vibrations of Asp, Asn, Glu, Gln, Lys, and Arg. NPY contains thirteen of these residues in the amino acid sequence (Fig. 1). The shortest NPY' fragment possesses only 5 these residues. This is why, in the RS spectrum of the acetyl-$(Leu^{28,31})$-NPY^{24-36} *C*-terminal fragment, the 933 cm^{-1} spectral feature due to ν(CC), ν(CN) and Tyr (ν_5) is as strong as the Tyr band at 959 cm^{-1} whereas the 959 cm^{-1} band of the full length NPY decreases, baring the His ring vibrations (at 988 cm^{-1}). The presence of His is also manifested (in RS spectra of all the investigated peptides) by the very weak ~1554 cm^{-1} Raman signal [ν(ring) + $\rho_{ipb}(N_1—H)$].

There are some other bands, which could be assigned to the aliphatic side-chain modes, especially of Arg, at 2934–2928 [ν_{as}(CH)], 2876 [ν_s(CH)], ~1460 [$\delta(CH_2)$], ~1446 [$\delta(CH_2)$ and/or δ(NH)],

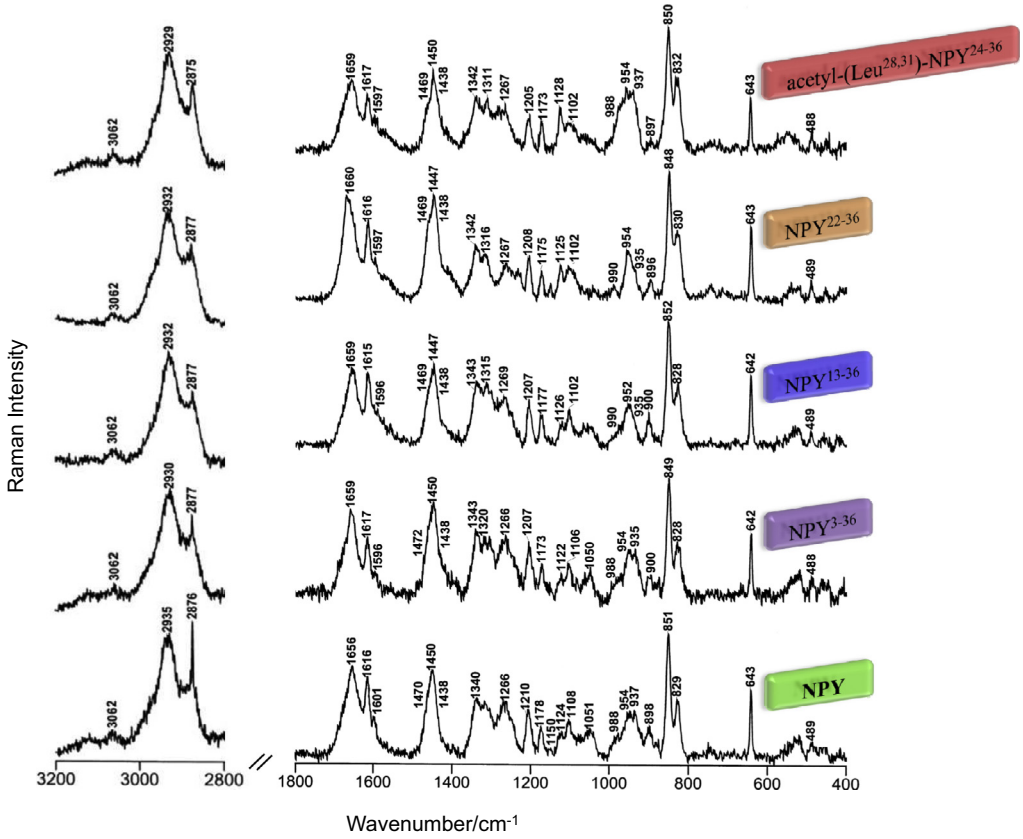

Fig. 4. The SERS spectra porcine NPY and its native NPY^{3-36}, NPY^{13-36}, and NPY^{22-36} and mutated acetyl-$(Leu^{28,31})$-NPY^{24-36} *C*-terminal fragments.

~1342 [$\rho_w(CH_2)$], ~1174 [$\rho_r(NH_2)/\rho_r(NH_3^+)$], 1126–1155 [$\rho_r(NH_2)$] and/or $\nu_{asym}(CCN)$], ~1105 [$\nu_{as}(CCN)$ and/or $\rho_t(NH_2)$], and 1055–1051 [Arg [$\rho_w(NH_3^+)$ and/or $\nu(CN)$] (see Table 1).

As can be seen, NPY dissolved in water exhibits amide I and III bands at 1652 and 1267 cm^{-1}, respectively [17]. The 1652 cm^{-1} Raman signal was interpreted to represent the α-helical or unordered structure, whereas the amide II mode was allocated to the β-turn structure. The spectra presented in Fig. 3 show the broad and asymmetric in shape 1656–1652 and ~1263 cm^{-1} amide bands that supports earlier result. This asymmetric shape is a consequence of overlapping of the amide modes with vibrations of different secondary structures and molecular fragments (Tyr, $\nu(C{=}N)$, $\rho_b(NH_2)/\rho_s(NH_2)$). This overlap is clearly seen in second-derivative spectra of the corresponding RS spectra that reveal several components in the amide I region. The wavenumbers and proposed assignments to the proper conformation for these second-derivative spectra are given in Table 2. For example, three signals at around 1678, 1660, and 1652 cm^{-1} (Table 2) were calculated for porcine NPY and its native NPY^{3-36}, NPY^{13-36}, NPY^{22-36}, and mutated acetyl-$(Leu^{28,31})$-NPY^{24-36} *C*-terminal fragments. The strongest signal at ~1652 cm^{-1} is due to the α-helical conformation. The ~1678 and ~1660 cm^{-1} bands arise from the turn and disordered arrangement of the peptide backbones.

Comparison of the SERS spectra in Fig. 4 reveals a striking similarity in the spectral patterns. This finding implies that the same molecular fragment(s) of all the investigated peptides interact(s) with the colloidal silver surface. Because, acetyl-$(Leu^{28,31})$-NPY^{24-36} is the shortest *C*-terminal fragment under investigation and there is no evidence that the acylation of Leu^{24} (lack of a 1380–1415 cm^{-1} SERS signal of a carboxyl group) and $Ile^{28,31} \rightarrow Leu^{28,31}$ substitution influence the SERS pattern; thus, it seems that the NPY^{32-36} *C*-terminal fragment (Thr^{32}–Arg^{33}–Gln^{34}–Arg^{35}–$Tyr^{36}NH_2$) is the common fragment of all the investigated peptides involved in the interaction with the silver nanoparticles. In Fig. 5 we proposed a possible manner of interaction between the investigated peptides and the silver nanoparticle surface. The discussion in the paragraph below confirms this scheme.

The SERS and RS spectra are quite similar. This is why the detailed band assignment discussed in the above paragraph is omitted here. However, some differences in the relative enhancement of some bands can be seen. For example, the ~1438 [$\delta(CH_2)$ chain deformation] and ~896 cm^{-1} [$\delta(CH_2)$, chain asymmetric stretch] Raman bands (Table 1) are decreased or absent in the SERS spectra. From the Raman signals in the spectral range of 800–400 cm^{-1}, the 643 cm^{-1} band remains only in the SERS spectra without change in the frequency (0–2 cm^{-1}) and band width. The totally symmetric *para*-substituted phenyl ring Raman mode (1204 cm^{-1}) loses the SERS relative intensity, moves down by 3–6 cm^{-1}, and slightly (3–6 cm^{-1}) broadness. Generally, the SERS spectral features between 1350 and 1250 cm^{-1}, caused by Tyr and Arg vibrations, and the $I_{830/850}$ ratio slightly decrease only in comparison to those in the RS spectra. Therefore, it can be stated that the Tyr and Arg residues are in contact with the silver nanoparticle surface. This is in accordance with previous studies that have demonstrated that a set of 1170, 1247, 1484, and 1595 cm^{-1} bands is characteristic for tyrosine-to-metal charge transfer excitation in a variety of metalloenzymes, where Tyr is coordinated to a metal ion [34,44]. On the other hand, the work of Hubbard et al. [45], based on the Tyr EELS bands; i.e., 1325 [$\rho_{ipb}(CH) + \nu_{trig}(CC)$, $\nu(CO)$], 1221 [$\rho(OH) + \nu(CO)$], and 1128 cm^{-1} [$\nu(CO)$, $\rho_{ipb}(CH)$, $\rho_{oopb}(CH)$], have shown that the Tyr ring preferentially adopts horizontal orientation in respect to the platinum surfaces. Two of the aforementioned spectral features, the ~ 1340 and ~1124 cm^{-1}, are enhanced in the SERS spectra of all

Table 1
Wavenumbers and proposed bands assignment for the RS and SERS spectra of porcine NPY and its native NPY^{3-36}, NPY^{13-36}, and NPY^{22-36} and mutated acetyl-$(Leu^{28,31})$-NPY^{24-36} *C*-terminal fragments.

Assignment	Wavenumber (cm^{-1})									
	NPY		NPY^{3-36}		NPY^{13-36}		NPY^{22-36}		Acetyl-$(Leu^{28,31})$-NPY^{24-36}	
	RS	SERS	RS	SERS	RS	SERS	RS	SERS	RS	SERS
Tyr [ν_{6a}]	434	437	433	443	435	447	434	447	431	440
ρ_{oopb}(CCC)	485	489	486	488	487	489	487	489	486	488
ρ_{oopb}(CCC)	597	–	595	–	595	–	597	–	596	–
Tyr [ν_{6b}]	641	643	641	642	642	642	641	643	641	643
Tyr [ν_4]	719	–	721	–	722	–	722	–	720	–
Tyr [ρ_b(ring)], Arg [$\rho_r(CH_2)$]	747	–	745	–	746	–	745	–	742	–
Tyr doublet (trigonal CCC bend)	829	829	829	828	827	828	829	830	829	832
Tyr doublet (CCC puckering)	849	851	849	849	849	852	847	848	848	850
Tyr [$\rho_r(C_\gamma H_2)$] and/or ν(CC) ring breathing	895	898	900	902	898	900	896	896	896	897
ν(CC), ν(CN), and/or Tyr(ν_5)	936	937	934	935	934	935	934	935	933	937
ν_{as}(CCC) and Tyr [ρ_{oopb}(CH)]	959	954	954	954	956	952	953	954	959	954
$\rho_r(CH_2)$	988	988	988	988	990	990	988	990	–	988
Arg [$\rho_w(NH_2)$], ν(CN), and/or $\rho_r(CH_2)$]	1055	1051	1051	1050	–	–	–	–	–	–
ν_{as}(CCN), $\rho_t(NH_2)$, and/or Tyr [ρ_w(CH)]	1105	1108	1103	1106	1105	1102	1103	1102	1105	1102
Tyr [ρ_{ipb}(CH), ρ_{oopb}(CH)], ν(CO)], Arg [$\rho_r(NH_2)$], ν_{asym}(CCN)	1126	1124	1125	1122	1124	1126	1125	1125	1126	1128
Arg [δ(NH)], Tyr ρ_{oopb}(CH)]	1153	1150	1153	1150	1155	1150	1151	1150	1151	1150
Tyr [ν_{9a}, ρ_{ipb}(CH) + $\nu(C_6H_5—C)$, Tyr [$\nu_{sym}(C_\beta\ C_\gamma H_2 C_\delta)$] and/or Arg [$\rho_r(NH_2)/\rho_r(NH_3^+)$]	1172	1178	1174	1173	1174	1177	1174	1175	1172	1173
Tyr [ν_{7a}, totally symmetric *para*-substituted phenyl]	1204	1210	1204	1207	1204	1207	1204	1208	1204	1205
Amide III and/or Tyr [δ_s(ring) + ν(CO)], Arg [$\rho_r(NH_2)$], $\rho_t(CH_2)$	1264	1266	1265	1266	1265	1269	1265	1267	1263	1267
Tyr [ν(CC), ν(CO), ρ_{ipb}(CH), ν(COH), and $\rho_w(CH_2)$]	1319	1320	1318	1320	1318	1315	1318	1316	1311	1311
Tyr [ρ_{ipb}(CH) + ν_{trig}(CC), ν(CO)] and/or $\rho_w(CH_2)$	1334	1340	1337	1343	1340	1343	1341	1342	1342	1342
$\delta(CH_2)$ and/or Arg [$\rho_{oopr}(NH_2)$],	1433	1438	1434	1438	1433	1438	1434	1438	1434	1438
Tyr [ν_{19b}]	1447	1450	1449	1450	1444	1447	1446	1447	1446	1450
Tyr [ν_{19a}] and/or $\delta(CH_2)$	1460	1470	1460	1472	1460	1469	1460	1469	1460	1469
Tyr [ν_{8b}]	1598	1601	1598	1596	1597	1596	1597	1597	1596	1597
Tyr [ν_{8a}]	1614	1616	1616	1617	1614	1615	1615	1616	1614	1617
Am I, $\rho_b(NH_2)/\rho_s(NH_2)$, and/or ν(C=N)	1654	1656	1652	1659	1656	1659	1656	1660	1655	1659
ν_s(CH)	2876	2876	2876	2876	2876	2876	2876	2876	2876	2876
ν_{as}(CH)	2934	2934	2934	2934	2934	2934	2932	2932	2928	2928
Tyr [$\nu(CH)_{ring}$]	3063	3062	3063	3062	3057	3062	3061	3062	3060	3062

Abbreviations: ν – stretching, δ – deformation, ρ_r – rocking, ρ_w – wagging, ρ_{ipb} – in-plane bending, ρ_{oopb} – out-of-plane bending, ρ_s – scissoring, s – symmetric, and as – asymmetric vibrations; Tyr – L-tyrosine, Arg – L-arginine.

Table 2
Calculated wavenumbers in the amide I region in the second-derivative RS and SERS spectra of porcine NPY and its native NPY^{3-36}, NPY^{13-36}, and NPY^{22-36} and mutated acetyl-$(Leu^{28,31})$-NPY^{24-36} *C*-terminal fragments.

Assignment	NPY		NPY^{3-36}		NPY^{13-36}		NPY^{22-36}		Acetyl-$(Leu^{28,31})$-NPY^{24-36}	
	RS	SERS	RS	SERS	RS	SERS	RS	SERS	RS	SERS
Tyr	1614^s	1616^s	1615^s	1615^s	1614^s	1615^s	1615^s	1615^s	1615^s	1616^s
Tyr	1598^m	1596^m	1596^m	1596^m	1596^m	1599^w	1596^m	1596^m	1595^m	1598^w
ν(C=N) and/or $\rho_b(NH_2)/\rho_s(NH_2)$	1633^w	1642^w	1640^w	1638^w	1649^w	1637^w	1642^w	1640^w	1637^w	1649^w
Am I										
Turn	1678^m	1677^w	1683^w	1676^w	1688^w	1689^w	1686^w	1689^w	1681^w	1685^w
Coil	1660^w	1664^w	1665^w	1661^w	1669^w	1676^w	1667^w	1665^m	1663^w	1665^w
α-Helix	1652^s	1655^s	1652^s	1656^s	1657^m	1650^m	1652^m	1654^m	1652^m	1655^m

Abbreviations: s – strong, m – medium, w – weak.

the investigated peptides. However, the 1221 cm^{-1} signal is absent, suggesting that upon adsorption Tyr undergoes deprotonation. This is in agreement with the data obtained for the Tyr-mutated bombesin 6–14 fragments [46]. One more fact supports the proposed parallel arrangement of the Tyr ring on the silver nanoparticle surface, i.e. the lack of the breathing ring vibration around 1000 cm^{-1}. Additionally, all of the SERS frequencies and widths of the Tyr ring modes observed for all the investigated peptides are only slightly shifted (by 0–3 cm^{-1}) and broadened (by 1–4 cm^{-1}) in comparison with those in the RS spectra. Therefore, the Tyr–O ring rather interacts with the silver nanoparticles than binds to its surface. It is worth stressing out, that the $I_{830/850}$ equals ca. 0.5 for NPY and NPY^{3-36} and negligibly increases in acetyl-$(Leu^{28,31})$-NPY^{24-36} ($I_{830/850}$ equals 0.6). This value confirms that the Tyr residue for all the investigated peptides is exposed to the silver surface.

Another important aspect of the proposed adsorption model of the investigated peptides concerns the guanidine group, *N*-terminal —NH_2 group, and amide bond vibrations. Without Undoubtedly, the strong broad ~1659 cm^{-1} and medium relative intensity ~1267 cm^{-1} SERS signals are due to the amide modes; however, they overlap with other bands as is evident from Table 2. The gap in the spectral range between 1415 and 1370 cm^{-1}, where the carbonyl vibrations are expected to appear, suggests that the ~1266, ~1178, ~1150, ~1108, and ~1051 cm^{-1} spectral features are due to the Arg residue oscillations rather than to the

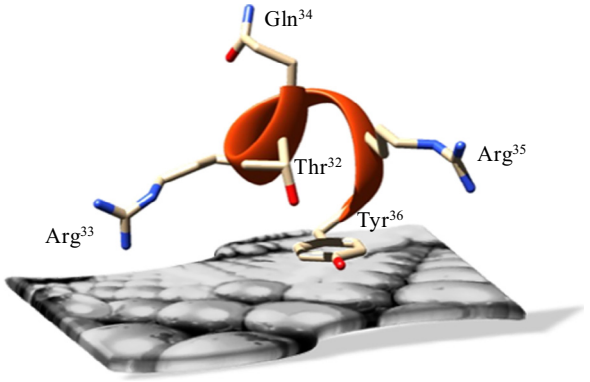

Fig. 5. The possible manner of the interaction of the porcine NPY$^{32-36}$ *C*-terminal fragment with the colloidal silver nanoparticle.

N-terminal —NH_2 modes. This can be supported by the second derivative spectra of all the investigated peptides that show the ~1652 cm^{-1} band allocated to the C=N bond stretches. Thus, based on the above observation it can be proposed that the amide bond closest to the *C*-terminal Tyr interacts with the silver surface, whereas the Arg residue only assists in the peptides interaction with this surface.

4. Conclusions

Based on the SERS spectra, we discussed the mode of adsorption of porcine NPY and its native NPY$^{3-36}$, NPY$^{13-36}$, and NPY$^{22-36}$ and mutated acetyl-(Leu^{28,31})-NPY$^{24-36}$ *C*-terminal fragments. The analysis of the adsorption geometry of these peptides was carried out based on the observed changes in the wavenumber, enhancement, and broadening of the corresponding Raman and SERS bands. We showed that the Tyr ring of all the investigated peptides, being parallel to the silver nanoparticles surface, rather interacted with this surface than bound to it. We suggested that the amide bond closest to the *C*-terminal fragment (Thr^{32}–Arg^{33}–Gln^{34}–Arg^{35}–Tyr^{36}NH_2) interacted with the silver substrate, whereas the Arg residue only assisted in the adsorption process. In addition, we demonstrated that the NPY$^{32-36}$ *C*-terminal part was responsible for the adsorption process at the silver nanoparticle/water interface. This is consistent with the earlier results for neuropeptide tyrosine NPY$^{13-36}$ in solution [26], which indicated that the *C*-terminus of NPY, especially Leu^{30}–Tyr^{36} molecular fragment, was the site engaged in the receptor binding. The agreement between evidence from our experiments, and NMR and molecular modeling studies [26] confirms our hypothesis about correlation between the structural component responsible for ability to interact with the Y_2 receptor and the silver colloidal surface, therefore, our present results shed a new light on the structure–function relationship of NPY and its analogues acting on the Y_2 receptors.

Acknowledgments

This work was supported by UJ/WCh/DS5 (Faculty of Chemistry, Jagiellonian University) and the postdoctoral project Interdisciplinary PhD Studies "Molecular Sciences for Medicine" (Project No. POKL.04.01.01-00-056/10 to H.D.) co-financed by the European Social Fund within the Human Capital Operational Program. Y. Kim gratefully acknowledges HUFS for financial support.

References

[1] B.M. Chronwall, D.A. DiMaggio, V.J. Massari, V.M. Pickel, D.A. Ruggiero, T.L. O'Donohue, Neuroscience 15 (1985) 1159–1181.
[2] S.A. Monks, G. Karagianis, G.J. Howlett, R.S. Norton, J. Biomol. NMR 8 (1996) 379–390.
[3] J.L. Krstenansky, T.J. Owen, S.H. Buck, K.A. Hagaman, L.R. McLean, Proc. Natl. Acad. Sci. USA 86 (1989) 4377–4381.
[4] M. Śmiałowska, H. Domin, Neuroprotective effects of neuropeptide Y and Y2 and Y5 receptor agonists in vitro and in vivo, in: L.M. Martins, S.H.Y. Loh (Eds.), Neurodegeneration, InTech, Rijeka, 2012, pp. 37–58.
[5] I. Merchenthaler, F.J. Lopez, A. Negro-Vilar, Proc. Natl. Acad. Sci. USA 87 (1990) 6326–6330.
[6] M.C. Michel, A. Beck-Sickinger, H. Cox, H.N. Doods, H. Herzog, D. Larhammar, R. Quirion, T. Schwartz, T. Westfall, Pharmacol. Rev. 50 (1998) 143–150.
[7] A. Bettio, A.G. Beck-Sickinger, Biopolymers 60 (2001) 420–437.
[8] M. Śmiałowska, H. Domin, B. Zieba, E. Koźniewska, R. Michalik, P. Piotrowski, M. Kajta, Neuropeptides 43 (2009) 235–249.
[9] C. Cabrele, M. Langer, R. Bader, H.A. Wieland, H.N. Doods, O. Zerbe, A.G. Beck-Sickinger, J. Biol. Chem. 275 (2000) 36043–36048.
[10] Y. Dumont, A. Cadieux, H. Doods, A. Fournier, R. Quirion, Can. J. Physiol. Pharmacol. 78 (2000) 116–125.
[11] R. Sankararamakrishnan, Biosci. Rep. 26 (2006) 131–158.
[12] M. Mousli, Y. Landry, Agents Actions 41 (1994) C41–C42.
[13] T.L. Blundell, J.E. Pitts, I.J. Tickle, S.P. Wood, C.W. Wu, Proc. Natl. Acad. Sci. USA 78 (1981) 4175–4179.
[14] C. Cabrele, A.G. Beck-Sickinger, J. Pept. Sci. 6 (2000) 97–122.
[15] J. Allen, J. Novotný, J. Martin, G. Heinrich, Proc. Natl. Acad. Sci. USA 84 (1987) 2532–2536.
[16] I.D. Glover, D.J. Barlow, J.E. Pitts, S.P. Wood, I.J. Tickle, T.L. Blundell, K. Tatemoto, J.R. Kimmel, A. Wollmer, W. Strassburger, et al., Eur. J. Biochem. 142 (1984) 379–385.
[17] A. Balasubramaniam, V. Renugopalakrishnan, D.F. Rigel, M.S. Nussbaum, R.S. Rapaka, J.C. Dobbs, L.A. Carreira, J.E. Fischer, Biochim. Biophys. Acta 997 (1989) 176–181.
[18] G. Jung, A.G. Beck-Sickinger, H. Dürr, W. Gaida, G. Schnorrenberg, Biopolymers 31 (1991) 613–619.
[19] M. Gurrath, A. Bisello, K. Bottazzo, C.W. Chung, S. Mammi, E. Peggion, J. Pept. Sci. 2 (1996) 176–193.
[20] A. Bettio, M.C. Dinger, A.G. Beck-Sickinger, Protein Sci. 11 (2002) 1834–1844.
[21] D.J. Cowley, J.M. Hoflack, J.T. Pelton, V. Saudek, Eur. J. Biochem. 205 (1992) 1099–1106.
[22] A.G. Beck-Sickinger, G. Jung, Biopolymers 37 (1995) 123–142.
[23] M. Lerch, V. Gafner, R. Bader, B. Christen, G. Folkers, O. Zerbe, J. Mol. Biol. 322 (2002) 1117–1133.
[24] R. Schwyzer, Biopolymers 31 (1991) 785–792.
[25] R. Bader, G. Rytz, M. Lerch, A.G. Beck-Sickinger, O. Zerbe, Biochemistry 41 (2002) 8031–8042.
[26] M. Labelle, S. St-Pierre, R. Savard, Y. Boulanger, Eur. J. Biochem. 246 (1997) 780–785.
[27] S. Siddhanta, C. Narayana, Nanomater. Nanotechnol. 2 (2012) 1–13.
[28] S.A. Overman, G.J. Thomas Jr., Biochemistry 34 (1995) 5440–5451.
[29] C. Xie, Y. Li, J. Appl. Phys. 93 (2003) 2982–2986.
[30] R. Tuma, J. Raman Spectrosc. 36 (2005) 307–319.
[31] N.C. Maiti, M.M. Apetri, M.G. Zagorski, P.R. Carey, V.E. Anderson, J. Am. Chem. Soc. 126 (2004) 2399–2408.
[32] K. Kneipp, H. Kneipp, I. Itzkan, R.R. Dasari, M.S. Feld, J. Phys. Condens. Matter. 14 (2002) R597–R624.
[33] E. Podstawka-Proniewicz, D. Sobolewski, A. Prahl, Y. Kim, L.M. Proniewicz, J. Raman Spectrosc. (2012) 51–60.
[34] E. Podstawka-Proniewicz, M. Kosior, Y. Kim, K. Rolka, L.M. Proniewicz, Biopolymers 93 (2010) 1039–1054.
[35] E. Podstawka-Proniewicz, A. Kudelski, Y. Kim, L.M. Proniewicz, J. Phys. Chem. B 115 (2011) 7079–7108.
[36] E. Podstawka-Proniewicz, A. Kudelski, Y. Kim, L.M. Proniewicz, J. Phys. Chem. B 115 (2011) 6709–6721.
[37] E. Podstawka, Y. Ozaki, L.M. Proniewicz, Appl. Spectrosc. 58 (2004) 1147–1156.
[38] D. Grandt, M. Schimiczek, W. Rascher, F. Feth, J. Shively, T.D. Lee, M.T. Davis, J.R. Reeve Jr., M.C. Michel, Regul. Pept. 67 (1996) 33–37.
[39] S. Yao, M.A. Smith-White, E.K. Potter, R.S. Norton, J. Med. Chem. 45 (2002) 2310–2318.
[40] M.C. Michel, A. Beck-Sickinger, H. Cox, H.H. Doods, H. Herzog, D. Larhammar, R. Quirion, T. Schwartz, T. Westfall, Pharmacol. Rev. 50 (1998) 143–150.
[41] K. Bobińska, J. Szemraj, T. Pietras, K. Zboralski, P. Gałecki, Psychaitr. Pol. 42 (2008) 889–901.
[42] M.N. Siamwiza, R.C. Lord, M.C. Shen, T. Takamatsu, I. Harada, H. Matsuura, T. Shimanouchi, Biochemistry 14 (1975) 4870–4876.
[43] H. Sugeta, A. Go, T. Miyazawa, Chem. Lett. 1 (1972) 83–86.
[44] E. Proniewicz, P. Pienpinijtham, Y. Ozaki, Y. Kim, L.M. Proniewicza, J. Raman Spectrosc. 44 (2013) 55–62.
[45] N. Batina, D.G. Frank, J.Y. Gui, B.E. Kahn, C.-H. Lin, F. Lu, J.W. McCargar, G.N. Salaita, D.A. Stern, D.C. Zapien, A.T. Hubbard, Electrochim. Acta 34 (1989) 1031–1044.
[46] E. Podstawka, Y. Ozaki, Biopolymers 89 (2008) 941–950.
[47] E. Podstawka, E. Sikorska, L.M. Proniewicz, B. Lammek, Biopolymers 83 (2006) 193–203.
[48] D. Sobolewski, E. Proniewicz, D. Skołuba, A. Prahl, Y. Ozaki, Y. Kim, L.M. Proniewicz, J. Raman Spectrosc. 44 (2013) 212–218.
[49] E. Podstawka-Proniewicz, N. Piergies, D. Skołuba, P. Kafarski, Y. Kim, L.M. Proniewicz, J. Phys. Chem. A 115 (2011) 11067–11078.

[50] E. Proniewicz, Y. Ozaki, Y. Kim, L.M. Proniewicz, J. Raman Spectrosc. 44 (2013) 355–361.
[51] E. Podstawka-Proniewicz, D. Sobolewski, A. Prahl, Y. Kim, L.M. Proniewicz, J. Raman Spectrosc. 43 (2012) 51–60.
[52] A. Brambilla, A. Philippidis, A. Nevin, D. Comelli, G. Valentini, D. Anglos, J. Mol. Struct. 1044 (2013) 121–127.
[53] S. Stewart, P.M. Fredericks, Spectrochim. Acta A 55 (1999) 1641–1660.
[54] S. Kumar, A. Kumar Rai, S.B. Rai, D.K. Rai, A.N. Singh, V.B. Singh, J. Mol. Struct. 791 (2006) 23–29.
[55] F.M. Almeida, P.T.C. Freire, R.J.C. Lima, C.M.R. Remédios, J. Mendes Filho, F.E.A. Melo, J. Raman Spectrosc. 37 (2006) 1296–1301.
[56] S. Kumar, A. Kumar Rai, S.B. Rai, D.K. Rai, Indian J. Phys. 84 (2010) 563–573.
[57] A.E. Aliaga, I. Osorio-Roman, C. Garrido, P. Leyton, J. Cárcamo, E. Clavijo, J.S. Gómez-Jeria, F.G. Díaz, M.M. Campos-Vallette, Vib. Spectrosc. 50 (2009) 131–135.
[58] E. Proniewicz, D. Skołuba, I. Ignatjev, G. Niaura, D. Sobolewski, A. Prahl, L.M. Proniewicz, J. Raman Spectrosc. 44 (2013) 655–664.
[59] A.E. Aliaga, C. Garrido, P. Leyton, F.G. Diaz, J.S. Gomez-Jeria, T. Aguayo, E. Clavijo, M.M. Campos-Valette, S. Sanchez-Cortes, Spectrochim. Acta A 76 (2010) 458–463.
[60] K.A. Guzzetti, A.B. Brizuela, E. Romano, S.A. Brandán, J. Mol. Struct. 1045 (2013) 171–179.
[61] G. Zhu, X. Zhu, Q. Fan, X. Wan, Spectrochim. Acta A 78 (2011) 1187–1195.
[62] J.T. López Navarrete, V. Hernández, F.J. Ramírez, J. Mol. Struct. 348 (1995) 249–252.